

Searching in the Forest for Local Bayesian Optimization

Difan Deng
Leibniz University Hannover

Marius Lindauer
Leibniz University Hannover

Abstract

Because of its sample efficiency, Bayesian optimization (BO) has become a popular approach dealing with expensive black-box optimization problems, such as hyperparameter optimization (HPO). Recent empirical experiments showed that the loss landscapes of HPO problems tend to be more benign than previously assumed, i.e. in the best case unimodal and convex, such that a BO framework could be more efficient if it can focus on those promising local regions. In this paper, we propose BOinG, a two-stage approach that is tailored toward mid-sized configuration spaces, as one encounters in many HPO problems. In the first stage, we build a scalable global surrogate model with a random forest to describe the overall landscape structure. Further, we choose a promising subregion via a bottom-up approach on the upper-level tree structure. In the second stage, a local model in this subregion is utilized to suggest the point to be evaluated next. Empirical experiments show that BOinG is able to exploit the structure of typical HPO problems and performs particularly well on mid-sized problems from synthetic functions and HPO.

1 Introduction

Hyperparameter optimization (HPO) is considered to be a tedious, error-prone and expensive problem, but nevertheless crucial for achieving peak performance of a machine learning algorithm on a given dataset (Bergstra and Bengio, 2012; Feurer and Hutter, 2019). Here we assume that a user-defined cost function f is optimized over a space \mathcal{X} of possible hyperparameter configurations $\mathbf{x} \in \mathcal{X}$: $\mathbf{x}^* \in \arg \min_{\mathbf{x} \in \mathcal{X}} f(\mathbf{x})$.

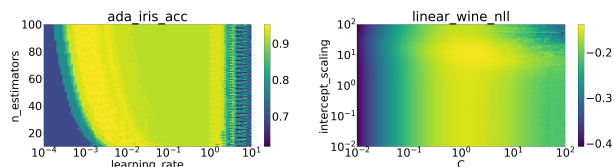


Figure 1: Exemplary hyperparameter loss landscape generated on BayesMark (Turner, 2019).

Typical cost functions f include, for example, accuracy for classification or RMSE for regression either over a hold-out validation set or a k -fold cross validation on the training set (Thornton et al., 2013). Since HPO is often treated as an expensive black-box problem, where only a few function evaluations can be afforded and no gradient is available, Bayesian Optimization (BO; (Jones et al., 1998)) is a common and efficient approach for obtaining well-performing hyperparameter configurations (Snoek et al., 2012; Hutter et al., 2012; Bergstra et al., 2013; Eriksson et al., 2019).

However, previous work on HPO showed two important insights: First, the loss landscape of a hyperparameter optimization problem is more benign than what one would expect (Klein et al., 2017; Pushak and Hoos, 2018; Pimenta et al., 2020). In most cases, the loss landscape in well-performing regions is quite flat and the best performing region is fairly well defined, see for example Figure 1. Given a limited HPO budget, we prefer to focus more on identified best performing regions and to avoid unnecessary exploration in the later stages of the optimization. Second, different surrogate models, used to trade-off exploration and exploitation, perform well depending on the task at hand (Eggensperger et al., 2013).

Inspired by recent advances in exploiting local structures in BO (Eriksson et al., 2019; Wang et al., 2020; Wan et al., 2021), we address these insights by proposing a two-stage BO algorithm. Our approach treats the optimization problem on different scales: in the first stage, i.e. the global level, we execute a full BO iteration with all observed points that are evaluated previously. Then we extract a subregion based on the trained surrogate model and the suggested point given

by the global optimizer. In the second stage, i.e. the local level, we perform another BO iteration with only the points inside the subregion and train a local surrogate model. Finally, we propose the sample to be evaluated next on the local model. Since we combine the best of two surrogates by extracting the subregion on the global level from a random forest (RF) and performing BO with a Gaussian Process (GP) inside this subregion, our robust HPO method is hence named as *Bayesian Optimization inside a Grove (BOinG)*.

Our contributions are as follows:

1. We propose the two-stage Bayesian Optimization approach BOinG that allows to locate a promising subregion that should be explored more.
2. By using a scalable global model (e.g., RF), BOinG reduces the computational burden on the local model (e.g., GP), which scales better to more iterations than vanilla GP-BO.
3. We propose to augment the local Gaussian Process with global data distribution such that the model captures the local loss landscape while preserving the influence of the global data distribution at minimal cost.
4. We show the robustness and state-of-the-art performance of BOinG on several synthetic functions and HPO benchmarks for deep learning and reinforcement learning.

2 Related Work & Background

Bayesian Optimization (BO) became a promising approach in solving expensive black-box functions (Shahriari et al., 2016). Recent progress on BO focuses on extending BO to large scale and high dimensional search space (Kandasamy et al., 2015; Wang et al., 2018; Eriksson et al., 2019; Wang et al., 2020). BO needs to employ a surrogate model to describe the possible data distribution of the target function. A GP model is the commonly utilized surrogate model. The predicted mean and variance of a GP for given configuration \mathbf{x} is given by

$$\mu(\mathbf{x}) = \mathbf{k}_*^T (\mathbf{K} + \sigma^2 \mathbf{I})^{-1} \mathbf{y} \quad (1)$$

$$\sigma^2(\mathbf{x}) = \mathbf{K}(\mathbf{x}, \mathbf{x}) - \mathbf{k}_*^T (\mathbf{K} + \sigma^2 \mathbf{I})^{-1} \mathbf{k}_* \quad (2)$$

where \mathbf{k}_* is the covariance vector between \mathbf{x} and all previous observations, while \mathbf{K} is the covariance matrix of all previously evaluated points.

One drawback of GPs is its $\mathcal{O}(n^3)$ -complexity for fitting the n previous observations and $\mathcal{O}(n^2)$ for predicting

means and variances at query points. Several approximate models such as sparse Gaussian processes (Candela and Rasmussen, 2005) have been proposed to alleviate this issue by only using a set of additional points as inducing points to approximate the data distributions. Sparse GP reduces the complexity to $\mathcal{O}(m^2 n)$ and $\mathcal{O}(mn)$ for fitting and predicting respectively, where m is the number of the inducing points. Additionally, the introduction of variational inference (Titsias, 2009) brings great benefit to training a sparse GP, e.g., one can optimize a sparse GP w.r.t. each points individually (Hensman et al., 2013), apply natural gradient (Salimbeni et al., 2018) for faster optimization, etc. However, in exchange, sparse GP leads to poor variance estimation that could mislead the optimizer (Shahriari et al., 2016). Despite its various complexity issues, GPs remain the most widely used surrogate model in BO frameworks.

An alternative surrogate model is a random forest (RF (Breimann, 2001; Hutter et al., 2011)). An RF predicts the mean and variance values from the empirical mean and variance of each individual tree’s predictions. Additionally, the tree structure allows it to easily deal with various data types as well as conditional hyperparameters, which is a common case in complex hyperparameter spaces. Still, RF’s empirical mean and variance predictions might cause poor variance estimation when extrapolation is required (Shahriari et al., 2016).

Partitioning the entire search space into several subregions with trees has been applied to reduce the computational complexity (Wang et al., 2018) or work with heteroscedasticity (Gramacy et al., 2004; Assael et al., 2014) problems. The inborn hierarchy structure of trees makes them especially suitable for selecting the region that satisfies our requirements (Wang et al., 2014). We follow the same idea in BOinG to build a single local model on the most promising subregion that is obtained by the trees in an RF model.

Similar to BOinG, TuRBO (Eriksson et al., 2019) maintains a local model and expands or shrinks the subregion based on the evaluated result of the suggested point. TuRBO expands the subregion if it finds a point that is better than the current one and shrinks the subregion if the suggested point is worse than the current best evaluated point. TuRBO discards all previously evaluated observations if the subregion shrinks to be smaller than a threshold. Thus, TuRBO does not make full use of the previous evaluations and might sample repeatedly in the same region. Furthermore, since the local model and the subregion controller do not get access to the information about the entire search space, TuRBO might discard a promising subregion too early and hence cannot dig deeper within a limited budget. In contrast, BOinG maintains a global model

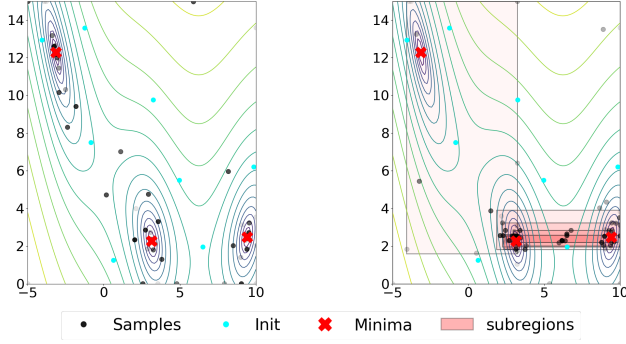


Figure 2: **Left:** The points suggested by a GP that is trained on the entire search space. **Right:** The subregions and points suggested by BOinG over time. Transparency visualizes subregions extracted in different phases.

and provides an estimation of the entire search space that guides the choice of the local subregion. Similarly, Wang et al. (2020) improved TuRBO by utilizing Monte Carlo Tree Search to guide the choice and size of the subregion. However, their method only restarts TuRBO in a similar manner as the method proposed in TuRBO. Thus their method might still waste too many resources until TuRBO restarts.

While TuRBO only considers BO as a local optimizer, McLeod et al. (2018) relies BO on finding the most promising subregion and only exploiting inside that subregion. BOinG considers the exploration and exploitation trade-off in both global and local levels. Hence it can quickly adjust to the local model while avoiding falling into local optimum too early.

3 A General Approach of Two-Stage Bayesian Optimization

Algorithm 1 outlines the general idea of BOinG. In each iteration, we first train a global surrogate model \hat{f}_g (Line 5) on all observations $\mathbf{X}^{(t-1)}$ to estimate the possible regions that are worth being explored. Using an acquisition function α_g on \hat{f}_g , we select a promising configuration (Line 6) that will guide the extraction of a subregion (Line 7; see Section 3.1 for details). Then a new local model \hat{f}_l is fitted to the observations inside the selected subregion $\mathbf{X}_{in}^{(t-1)}$ (see Section 3.2 for details). Based on \hat{f}_l , the maximum of a local acquisition function α_l (Line 9) decides the next configuration to be evaluated on the real cost function f (Line 10).

To be applicable to more complex problems with more reasonable evaluation budgets T , the global model needs to scale well to many observations, e.g., an RF is suitable (Hutter et al., 2011). Since the number of

Algorithm 1: Two-stage Bayesian Optimization with BOinG

- 1: **Input:** a black-box function f ; search space \mathcal{X} ; predictive models \hat{f}_g and \hat{f}_l that fit global and local observation distributions respectively; acquisition functions α_g and α_l ; evaluation budget T
 - 2: **Output:** global minimizer of f :
 $\mathbf{x} \in \arg \min_{\mathbf{x} \in \mathcal{X}} f(\mathbf{x})$
 - 3: **Initialization:** Initialize data $\mathbf{X}^{(0)}$ with initial observations
 - 4: **for** $t = 1, 2, \dots, T$ **do**
 - 5: fit global model $\hat{f}_g^{(t)}$ on $\mathbf{X}^{(t-1)}$
 - 6: select a candidate point \mathbf{x}_g with global acquisition function α_g :
 $\mathbf{x}_g \in \arg \max_{\mathbf{x} \in \mathcal{X}} \alpha_g(\mathbf{x}; \mathbf{X}^{(t-1)}, \hat{f}_g^{(t)})$
 - 7: extract a subregion $\mathcal{X}_{sub} \subseteq \mathcal{X}$ based on global candidate \mathbf{x}_g and model $\hat{f}_g^{(t)}$
 - 8: fit local model \hat{f}_l with the points inside the subregion $\mathbf{X}_i^{(t-1)} \in \mathcal{X}_{sub}$ together with the points outside the subregion
 $\mathbf{X}_o^{(t-1)} = \mathbf{X}^{(t-1)} \setminus \mathbf{X}_i^{(t-1)}$
 - 9: determine final sampling point based on local acquisition function α_l :
 $\mathbf{x}^{(t)} \in \arg \max_{\mathbf{x} \in \mathcal{X}_{sub}} \alpha_l(\mathbf{x}; \mathbf{X}_i^{(t-1)}, \mathbf{X}_o^{(t-1)}, \hat{f}_l^{(t)})$
 - 10: query $y^{(t)} := f(\mathbf{x}^{(t)})$
 - 11: update data: $\mathbf{X}^{(t)} \leftarrow \mathbf{X}^{(t-1)} \cup \{(\mathbf{x}^{(t)}, f(\mathbf{x}^{(t)}))\}$
 - 12: **end for**
 - 13: **Return:** $\hat{\mathbf{x}} \in \arg \min_{\mathbf{x} \in \mathcal{X}} f(\mathbf{x})$
-

points inside the subregion is rather small and nearly constant to some degree, we can afford the cost of accurate but expensive models (e.g., a GP) even if the number of the total evaluated points increases by a high degree.

Figure 2 (right) illustrates how the subregion and the suggested points vary during the optimization. As the optimization progresses, the subregion extracted by the global model gradually shrinks toward a potential optimum. BOinG mostly focuses on the regions that look promising—here the lower part of the figure—and invests more evaluations inside these regions to focus the exploration of the landscape. Please note that here BOinG hardly explores the region that is shown to be sub-optimal (the upper and right part of the image). It only takes a few evaluations in the beginning to indicate the unfitness of that region. As a comparison, the GP being trained on the entire space invests many evaluations on sub-optimal regions; even worse, the GP suggests lots of points on the boundary; see Figure 2 (left). BOinG hence focuses more on the regions that seem to be more promising. Thus, there is a good

chance for our method to find a better solution within a limited budget.

3.1 Subregion Extraction with RF

We build the global model on all previous observations and then select the most promising region to be exploited in the next stage. We propose to leverage the scalable and hierarchical structure of a tree-based model, such as an RF, s.t. we can split the global search space into subregions that contain sufficient data points to fit a local model.

First, we do a single BO iteration to determine a global candidate \mathbf{x}_g based on a global model \hat{f}_g and acquisition function α_g . Then starting from the root node of each tree and a subregion $\mathcal{X}_{sub} = \mathcal{X}$, we iterate toward the leaf node that contains \mathbf{x}_g and get a split of the current node. Each split will shrink \mathcal{X}_{sub} and exclude several points from \mathbf{X}_{in} . We repeatedly continue the split until it contains at least n_{min} points. We stop further exploring one node if that split makes the number of the points in the subregion smaller than n_{min} . Finally we stop shrinking the subregion if we cannot step further in any of the trees without keeping the number of the points in the subregion greater than n_{min} . For the corresponding algorithm, we refer to the appendix ??.

We illustrate a minimal toy example in Figure 3. We train an RF with two trees which split the space accordingly. Suppose that at least $n_{min} = 3$ points are required to be included in the subregion and the subregion grows from \mathbf{x}_g (marked in red). We note that, here \mathbf{x}_g is not an actual sampled point, but it only indicates the position that the subregion should contain. We first step from a_0 to a_2 as it contains \mathbf{x}_g and hence D and E are excluded from the subspace. Then we split the subspace with the split of b_0 , where all the points are preserved. We further go deeper into the first tree and arrive at node a_3 , in which case only 3 points lay in the subregion and we stop exploiting tree A. However, for tree B, as each split will not further shrink the subregion or exclude the existing points from the subregion, we arrive at leaf node b_5 and stop further shrinking the subregion.

One common issue arising from local BO is the size of the subregion. This region should not be too large, otherwise we would revert to a global optimization again. On the other hand, if the region is too small, the global optimum might be excluded from the subregion and we might only find a local minimum. Furthermore, the size of the subregion needs to be adapted to the number of the previous observations. A local optimizer should ideally contain all the previously evaluated points in the beginning and then gradually shrink to regions that are more likely to contain the global optimum. BOinG

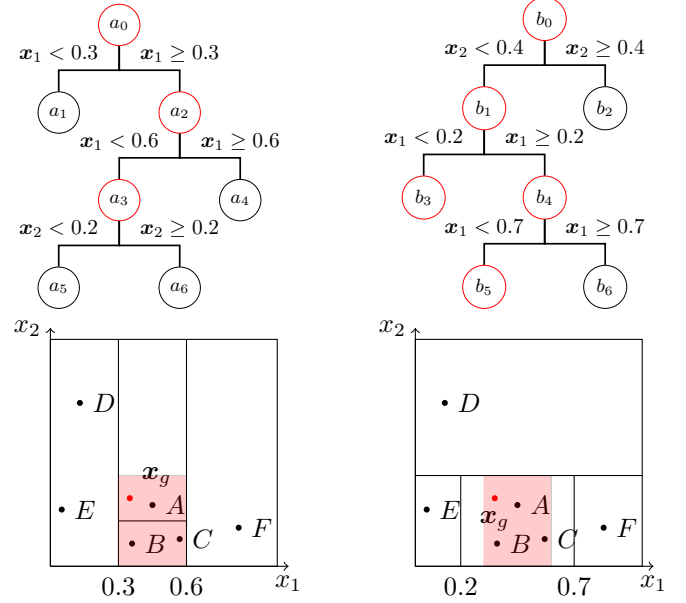


Figure 3: Subregion selection. The final extracted subregion is illustrated in the red-shaded region.

achieves this by its user-defined hyperparameter n_{min} . If the n_{min} points in the subregion are far from each other, i.e., BOinG still explores a lot and is not certain about a promising region, the selected subregion will be fairly large. In contrast if the n_{min} points in the subregion are near to each other, i.e., BOinG has already found a promising region, the selected subregion will be fairly small.

3.2 Fit Sub-Region with Gaussian Process

The global model suggests a subregion that is worth being further explored. We could then utilize a GP on the points inside the subregion as an accurate model to describe the local data distribution. However, this could lead to proposed points on the boundaries of the subregion again, since it does not capture the overall trend of the data. So, a compromise between fitting a GP on all observations and on only the observations inside the subregion is required. To this end, we propose a local GP with an augmentation of the global trend that fits all points within the subregion and in addition efficiently approximates the global data distribution.

We denote the points in the subregion and their function values as \mathbf{X}_i and \mathbf{f}_i ; here i refers to "inside subregions". Similarly we abbreviate the points outside the subregion as \mathbf{X}_o and \mathbf{f}_o respectively). Training a GP with \mathbf{X}_i and \mathbf{f}_i implicitly assumes that the prior distribution of \mathbf{f}_i follows $p(\mathbf{f}_i) = \mathcal{N}(\mathbf{0}, \mathbf{K}_{i,i})$; on the contrary, when a GP model is built to fit all the previous

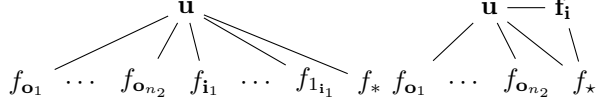


Figure 4: A comparison between FITC (left) and LGPGA (right). In FITC, test latent function values f_* can only obtain the information of \mathbf{f} through the inducing variable \mathbf{u} . While in LGPGA, f_* can directly obtain information from the information from \mathbf{f}_i .

evaluated points, \mathbf{f}_o provides a prior for \mathbf{f}_i :

$$p(\mathbf{f}_i|\mathbf{f}_o) = \mathcal{N}(\mu_{\mathbf{f}_i|\mathbf{f}_o}, \sigma_{\mathbf{f}_i|\mathbf{f}_o}^2) \quad (3)$$

$$\mu_{\mathbf{f}_i|\mathbf{f}_o} = \mathbf{k}_{o,i}^T (\mathbf{K}_{o,o} + \sigma^2 \mathbf{I})^{-1} \mathbf{y}_o \quad (4)$$

$$\sigma_{\mathbf{f}_i|\mathbf{f}_o}^2 = \mathbf{K}_{i,i} - \mathbf{k}_{o,i}^T (\mathbf{K}_{o,o} + \sigma^2 \mathbf{I})^{-1} \mathbf{k}_{o,i} \quad (5)$$

However, computing the posterior distribution with Equation 4 and 5 for \mathbf{X}_i is expensive and inefficient if we aim for higher evaluation budgets. Luckily, we can make use of the fact that the number of \mathbf{X}_o is much greater than the \mathbf{X}_i and most of \mathbf{X}_o are far away from the subregion and thus have little influence on the subregion. Thus, we approximate Equation 3 with a much cheaper proxy: a Sparse GP (Candela and Rasmussen, 2005).

Sparse GPs introduce a set of latent variables u called **inducing points** so that training points \mathbf{x} and test points \mathbf{x}_* are conditionally independent given u . We apply the same idea to approximate the posterior in Equation 4 and 5 and compute the posterior as a prior for $p(\mathbf{f}_i|\mathbf{f}_o)$. Since the local GP model is augmented with a globally approximated distribution, our model is dubbed Local GP with Global Augmentation (LGPGA).

We illustrate the difference between FITC (Snelson and Ghahramani, 2006)) on all observations and our LGPGA with an approximation of the global trend and exact fit of the points inside the subregion in Figure 4.

The joint distribution of LGPGA is then computed in the following way, in this work, we apply FITC to approximate the global trend:

$$\begin{bmatrix} \mathbf{f}_o \\ \mathbf{f}_i \\ \mathbf{f}_* \end{bmatrix} \sim \mathcal{N} \left(\mathbf{0}, \begin{bmatrix} \mathbf{Q}_{o,o} - \text{diag}[\mathbf{Q}_{o,o} - \mathbf{K}_{o,o}] & \mathbf{Q}_{o,i} & \mathbf{Q}_{o,*} \\ \mathbf{Q}_{i,o} & \mathbf{K}_{i,i} & \mathbf{K}_{i,*} \\ \mathbf{Q}_{*,o} & \mathbf{K}_{*,i} & \mathbf{K}_{*,*} \end{bmatrix} \right) \quad (6)$$

Where $\mathbf{Q}_{a,b}$ is defined as $\mathbf{K}_{a,u} \mathbf{K}_{u,u}^{-1} \mathbf{K}_{u,b}$ (Candela and Rasmussen, 2005).

Two sets of LGPGA hyperparameters need to be optimized: the kernel hyperparameters and the position of inducing points. Comparing with inference time, we optimize these two sets of hyperparameters in an inverse order: we first train a GP model to fit \mathbf{f}_i to get

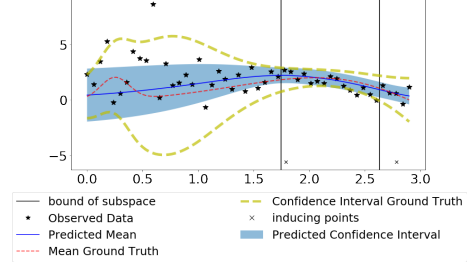


Figure 5: A LGPGA is utilized to fit the data points inside the subregion and still model the overall data trend also at the subregion’s boundaries.

the optimized kernel hyperparameters; thus LGPGA captures the local data distribution inside the subregion. We then train a sparse GP to fit \mathbf{f}_o . The kernel hyperparameters of this sparse GP are the same as the ones in the first stage and frozen during the training process. In which case the sparse GP only optimizes the position of the inducing points. Any existing approximating strategy can be applied in the second training stage (Titsias, 2009; Hensman et al., 2013; Salimbeni et al., 2018).

As illustrated in Figure 5, LGPGA is able to model the data in the subregion accurately. Additionally, on the right side of the subregion, LGPGA model takes the points outside the subregion into consideration and gives a more accurate prediction than a GP that only fits the data points inside the subregion. We note here, unlike previous work such as BOCK (Oh et al., 2018) that explicitly assumes that the optimal points are likely to be located in the center of the subregion, LGPGA does not make any assumption about the data distribution inside the subregion. Indeed, if the data points indicate that the boundary is still worth being explored, LGPGA would still try to sample the points near or on the boundary.

3.3 BOinG+: BOinG with Local TuRBO for Huge Budgets

Since RFs can have poor uncertainty estimates, SMAC (Lindauer et al., 2021) adds additional exploration by randomly sampling a new point with a certain probability and thus can provably converge to the true optimum in the limit (Hutter et al., 2011). In BOinG, we can also combine SMAC’s approach with the more explorative strategy of TuRBO: if we cannot make further progress with BOinG, we gradually increase the probability of switching to TuRBO instead of sticking to the subregion proposed by RF. To avoid unnecessary exploration, similar to Wang et al. (2020), we only do a TuRBO search inside a subregion, i.e. we randomly sample several points from \mathcal{X} and extract the subre-

regions \mathcal{X}_{sub} around them with the method proposed in Section 3.1. Since we are interested in stronger exploration, we then select the subregions with the largest volume and thus with the smallest density of observed points. Then we start a new TuRBO run within this subregion whose initial points are the existing points in this subregion. Similarly, if we cannot make further progress with TuRBO, we increase the probability of switching back to BOinG. As we employ BOinG as an exploitation mechanism, we restart TuRBO earlier to allow more exploration: TuRBO restarts if the length of its subregion is smaller than 2^{-7} , we restart TuRBO if its length is smaller than 2^{-4} . For the details, we refer to the appendix ??.

All in all, BOinG (and BOinG+) is introduced to alleviate the weakness of an RF model: RF is a poor extrapolator and might fail to estimate the data distribution correctly in the regions with lower density of evaluated points (Shahriari et al., 2016). Thus we build another GP model in the vicinity of the point suggested by RF with lower evaluated budgets. Because of the poor extrapolation abilities, we extend BOinG by random search with a model-guided optimizer (TuRBO) for larger budgets where we can afford and potentially need better exploration.

4 Experiments

In this section, we first evaluate BOinG on several different functions and then perform an ablation study.

Experimental Setup For the number of included points of a subregion based on an RF, we use $n_{min} := 5 \cdot d$, where d is the number of dimensions of the target function. The local model is a GP with Matérn 5/2-kernel. We set the number of inducing points $n_u := \min(10, 2 \cdot d)$. Further implementation details can be found in the appendix ??.

As a baseline, we compare BOinG with RF and a GP that is trained on all the previous evaluations. Both BOinG and full GP are implemented with GPyTorch v.1.2.1 (Gardner et al., 2018; Balandat et al., 2020). RF and acquisition function optimizers of the above-mentioned BO models are implemented in the framework of SMAC3 v1.0.1 (Hutter et al., 2012; Lindauer et al., 2021)¹, where a combination of random and local search for the optimization of the acquisition function is implemented.

Since TuRBO² and LA-MCTS³ are based on a similar idea of leveraging subregions, we compare BOinG

against these, using their original implementations. LA-MCTS provides two ways of doing local optimization: BO and TuRBO; we present both approaches in our experiments, dubbed LAMCTS-BO and LAMCTS-TuRBO. TuRBO allows for batch BO; however, for a fair comparison, we only evaluate TuRBO-1 and set its batch size to 1.

Furthermore, as baselines, we also compare against BO with GPs (GP) and RFs (RF) as surrogate models with EI (Jones et al., 1998) as acquisition function, and random search, using SMAC3. Finally, we consider TPE (Bergstra et al., 2011) as another baseline. SMAC implemented LogEI to model heavy-tailed cost distributions (Lindauer et al., 2021), our global optimizer follows the same implementation for HPO problems.

We ran all methods multiple times with different random seeds on 4 Intel Xeon E5 cores running openSUSE Leap 15.1. To ensure reproducibility, our code is publicly available at https://github.com/dengdifan/SMAC3/tree/boing_tmp

4.1 Synthetic Function

We assessed the algorithms on the following functions: Branin (2D), Ackley (10D) and Levy (10D).

Branin, as probably the most studied function in GP-BO, has 3 global optima. State-of-the-art BO methods can very well pin-point one of the optima, which lie within fairly narrow regions — unlike the landscape we expect for most HPO problems. Ackley has many local minima, allowing us to check against premature convergence. Levy has a large flat region near the optimum hence it tests the performance of an optimizer on a plateau. The input domain follows the suggestions in Surjanovic and Bingham (2013). All the optimization processes are repeated $30 \times$. These synthetic functions usually do not fit the requirement of "heavy-tailed cost distributions". We simply apply EI acquisition function instead of logEI on these functions.

Figure 6 shows that—as one might expect—GP-BO is a very strong approach for the Branin and Levy function, while on the Ackley function, the GP is not able to capture the high-dimensional, complex landscape well, and is outperformed by other approaches. Among all the compared optimizers, BOinG is the only one showing a robust performance on higher-dimensional problems, being always at least on par with the best optimizer.

4.2 Hyperparameter Optimization of ML Algorithms

Although synthetic functions are a nice sanity check, we designed BOinG with HPO in mind and thus evaluated

¹<https://github.com/automl/SMAC3>

²<https://github.com/uber-research/TuRBO>

³<https://github.com/facebookresearch/LaMCTS/tree/master/LA-MCTS>

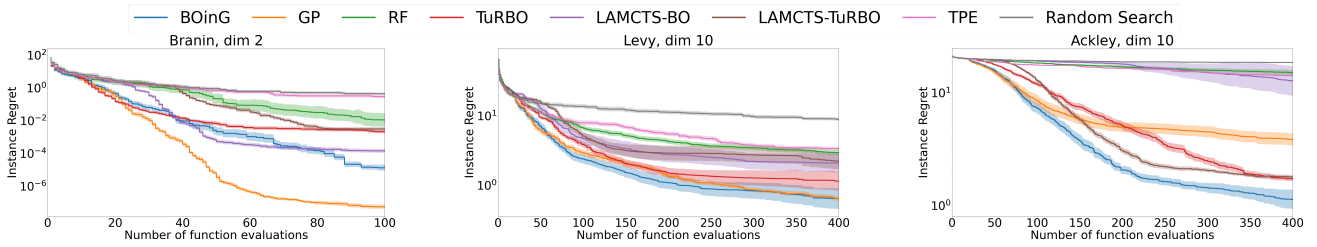


Figure 6: Optimization on different synthetic functions, the solid lines are the mean of the best observed values with semi-transparent areas to indicate standard error.

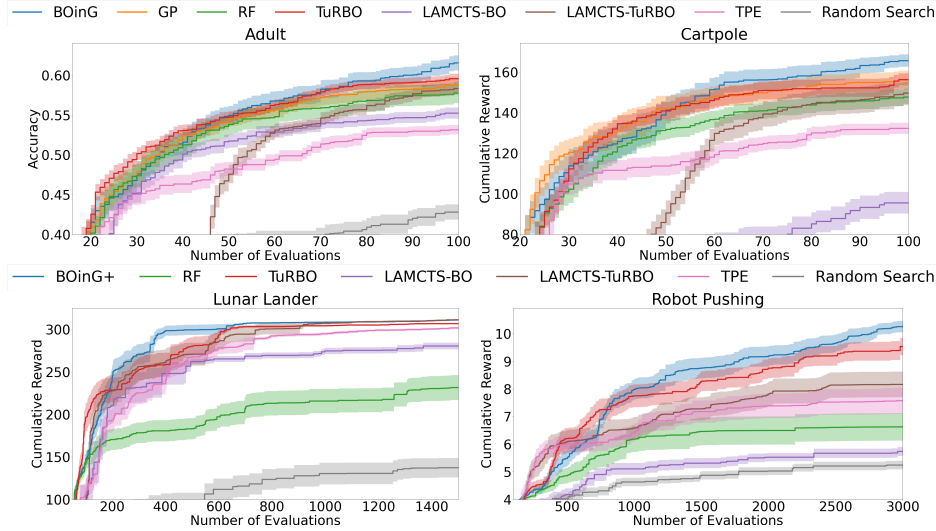


Figure 7: Results on ParamNet (Top Left), CartPole (Top Right), Lunar (Bottom Left) and Robot (Bottom Right). We show the mean performance and the standard error. Larger is better.

it on several HPO tasks.

We utilize BOinG to optimize the following hyperparameter benchmarks introduced by Falkner et al. (2018), provided by HPOBench (Eggenberger et al., 2021)⁴: (i) Tuning hyperparameter of a neural network surrogate model (ParamNet) for the Adult dataset (Adult) with eight hyperparameters; (ii) Tuning seven hyperparameters of proximal policy optimization (PPO) (Schulman et al., 2017) to learn the cartpole task. The PPO agent is implemented by Tensorforce (Kuhnle et al., 2017) and the environment is implemented in OpenAI gym (Brockman et al., 2016). For the details, we refer to the appendix ??.

Figure 7 (top) shows the result of different optimizers on both target algorithms. BOinG achieves substantially better final performance on both benchmarks. Since BOinG shares the same model as a full GP model in the beginning of the optimization phases ($5 \cdot d$), it achieves nearly the same performance as a full GP in the first few iterations and is able to identify the most promising region after ≈ 60 function evaluations.

Additionally, as BOinG introduces a local model to

reduce the complexity and BOinG+ solves the poor-extrapolator issue by RF, we could now study how BOinG scales to problems with larger budgets. We optimize 12 hyperparameters of a heuristic controller for a lunar lander implemented in the OpenAI gym and 14 hyperparameters of a controller for the robot pushing problem (Wang et al., 2018). The results are shown in the lower part of Figure 7. Although TuRBO and LA-MCTS-TuRBO are able to gain some advantage in the beginning, BOinG+ is able to catch up and even outperforms TuRBO and LA-MCTS-TuRBO after 200 function evaluations on Lunar Lander. On the robot benchmark, BOinG+ and TuRBO clearly outperform all the other methods, with a small advantage for BOinG+. Overall, the results show the strong performance of BOinG even in the large-budget setting.

4.3 Ablation Study

Here we evaluate how different design choices affect the performance of BOinG. Further ablation studies can be found in the appendix ??.

⁴<https://github.com/automl/HPOBench/>

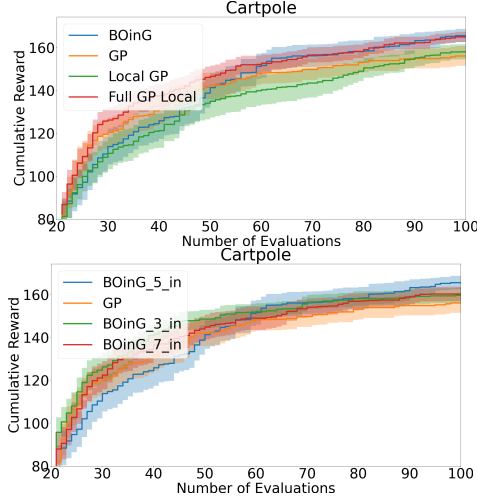


Figure 8: Ablation Study on LGPGA (Top) and n_{min} (Bottom).

4.3.1 LGPGA vs. GP

We study the extra benefit that a LGPGA brings to BOinG. In addition to LGPGA, we train a GP model only with the evaluations inside the subregion (*local GP*) and another GP model that is trained with all previous evaluations but the candidates are restrained to be selected from the subregion (*full GP local*). We evaluate the local GP models on the cartpole problem.

The result is shown in the left part of Figure 8. Both LGPGA and *full GP local* has better final performances compared to a *local GP*. However, consider the potential benefit that a LGPGA can bring (it requires less resources), we still suggest to use LGPGA in BOinG.

4.3.2 Number of points inside subregion

BOinG introduces a special hyperparameter: n_{min} , the number of points inside the subregion. n_{min} determines the size of the subregion to be explored in the next stage. Setting this value larger (e.g. to infinity) makes BOinG closer to a GP and thus requires more resources; reducing this value (e.g. until 0) leads BOinG to behave as an RF. As RF is often considered as a poor extrapolator, a BOinG with a small subregion might easily fall into a local minimum. Here we do an ablation study on n_{min} : *BOinG_ i _in* denotes a BOinG Optimizer that contains at least $i \cdot d$ points inside its subregion. *BOinG_3_in* achieves a better reward in the beginning but is then surpassed by *BOinG_5_in*; *BOinG_7_in* only starts to outperform a vanilla GP after ≈ 60 evaluations, which might be too late for a problem with 100-evaluation. We consider $5 \cdot d$ as a plausible number of points kept in the subregion.

5 Limitations

Even though BOinG is a robust approach, i.e. combining the best of GP-BO and RF-BO, GP-BO is often still the most efficient approach in low dimensional spaces. Furthermore, in higher dimensional spaces BO frameworks tend to suggest points near the boundary (Oh et al., 2018) of the configuration space. Such points might not give the RF enough insights about how to extract a subregion, i.e., the subregion might still be too close to the boundary. Last but not least, BOinG’s combination of two surrogate models and two acquisition functions might be brittle in some applications; however in our experiments BOinG turned out to be surprisingly robust across different tasks.

6 Discussion and Outlook

In this paper, we proposed BOinG, a hierarchical approach that combines the best of a random forest on a global optimization level and a Gaussian Process on a local level. The underlying idea is that BOinG can better focus on promising subregions by having better local models and pinpoint the optimum with fewer function evaluations. Empirical experiments show that BOinG is a very robust approach and is able to outperform vanilla BO and other local BO approaches on HPO problems. Although we focused on RFs and GPs as upper and lower level surrogate models, BOinG can also be seen as a model-agnostic approach, which could adopt other surrogate models, such as TPE. In future work, we plan to study whether we can benefit from a data density estimation approach such as TPE or non-axis-aligned splits (Wang et al., 2020) for better guidance on the upper level. Another promising approach would be to combine Thompson sampling for BO (Kandasamy et al., 2018) while maintaining multiple subregions (Eriksson et al., 2019) to perform batched BOinG efficiently.

7 Broader Impact

BO is often applied for solving expensive black-box function optimization where each single evaluation consumes lots of resources. Experiments show that our method achieves a better anytime performance on different HPO problems and thus consumes less resources in the evaluation phases. Additionally, the introduction of LGPGA reduces the potential resource consumption in the optimization overhead. Furthermore, BOinG contributes to automated machine learning (AutoML) and thus to democratizing machine learning, with all its benefits and risks. Since we do not address any specific application, we do not expect any conflict with general ethical conduct.

References

- Assael, J., Wang, Z., and Freitas, N. (2014). Heteroscedastic treed bayesian optimisation. *CoRR*, abs/1410.7172.
- Balandat, M., Karrer, B., Jiang, D. R., Daulton, S., Letham, B., Wilson, A. G., and Bakshy, E. (2020). BoTorch: A Framework for Efficient Monte-Carlo Bayesian Optimization. In *Advances in Neural Information Processing Systems 33*.
- Bergstra, J., Bardenet, R., Bengio, Y., and Kégl, B. (2011). Algorithms for hyper-parameter optimization. In Shawe-Taylor, J., Zemel, R., Bartlett, P., Pereira, F., and Weinberger, K., editors, *Proceedings of the 25th International Conference on Advances in Neural Information Processing Systems (NeurIPS’11)*, pages 2546–2554.
- Bergstra, J. and Bengio, Y. (2012). Random search for hyper-parameter optimization. *Journal of Machine Learning Research*, 13:281–305.
- Bergstra, J., Yamins, D., and Cox, D. (2013). Making a science of model search: Hyperparameter optimization in hundreds of dimensions for vision architectures. In Dasgupta, S. and McAllester, D., editors, *Proceedings of the 30th International Conference on Machine Learning (ICML’13)*, pages 115–123. Omnipress.
- Breimann, L. (2001). Random forests. *Machine Learning Journal*, 45:5–32.
- Brockman, G., Cheung, V., Pettersson, L., Schneider, J., Schulman, J., Tang, J., and Zaremba, W. (2016). OpenAI Gym. *arXiv:1606.01540 [cs.LG]*.
- Candela, J. and Rasmussen, C. (2005). A unifying view of sparse approximate gaussian process regression. *J. Mach. Learn. Res.*, 6:1939–1959.
- Dy, J. and Krause, A., editors (2018). *Proceedings of the 35th International Conference on Machine Learning (ICML’18)*, volume 80. Proceedings of Machine Learning Research.
- Eggenberger, K., Feurer, M., Hutter, F., Bergstra, J., Snoek, J., Hoos, H., and Leyton-Brown, K. (2013). Towards an empirical foundation for assessing Bayesian optimization of hyperparameters. In *NeurIPS Workshop on Bayesian Optimization in Theory and Practice (BayesOpt’13)*.
- Eggenberger, K., Müller, P., Mallik, N., Feurer, M., Sass, R., Klein, A., Awad, N., Lindauer, M., and Hutter, F. (2021). Hpobench: A collection of reproducible multi-fidelity benchmark problems for hpo.
- Eriksson, D., Pearce, M., Gardner, J., Turner, R., and Poloczek, M. (2019). Scalable global optimization via local bayesian optimization. In *Advances in Neural Information Processing Systems*, volume 32, pages 5496–5507.
- Falkner, S., Klein, A., and Hutter, F. (2018). BOHB: Robust and efficient hyperparameter optimization at scale. In Dy and Krause (2018), pages 1437–1446.
- Feurer, M. and Hutter, F. (2019). Hyperparameter optimization. pages 3–38. Springer. Available for free at <http://automl.org/book>.
- Gardner, J., Pleiss, G., Weinberger, Q., Bindel, D., and Wilson, A. (2018). Gpytorch: Blackbox matrix-matrix gaussian process inference with gpu acceleration. In *Advances in Neural Information Processing Systems*, volume 31, pages 7576–7586. Curran Associates, Inc.
- Gramacy, R., Lee, H., and Macready, W. (2004). Parameter space exploration with gaussian process trees. In Greiner, R., editor, *Proceedings of the 21st International Conference on Machine Learning (ICML’04)*, pages 45–52. Omnipress.
- Hensman, J., Fusi, N., and Lawrence, N. D. (2013). Gaussian processes for big data. In *Proceedings of the Twenty-Ninth Conference on Uncertainty in Artificial Intelligence, UAI’13*, page 282–290, Arlington, Virginia, USA. AUAI Press.
- Hutter, F., Hoos, H., and Leyton-Brown, K. (2011). Sequential model-based optimization for general algorithm configuration. In Coello, C., editor, *Proceedings of the Fifth International Conference on Learning and Intelligent Optimization (LION’11)*, volume 6683 of *Lecture Notes in Computer Science*, pages 507–523. Springer.
- Hutter, F., Hoos, H., and Leyton-Brown, K. (2012). Parallel algorithm configuration. In Hamadi, Y. and Schoenauer, M., editors, *Proceedings of the Sixth International Conference on Learning and Intelligent Optimization (LION’12)*, volume 7219 of *Lecture Notes in Computer Science*, pages 55–70. Springer.
- Jones, D., Schonlau, M., and Welch, W. (1998). Efficient global optimization of expensive black box functions. *Journal of Global Optimization*, 13:455–492.
- Kandasamy, K., Krishnamurthy, A., Schneider, J., and Póczos, B. (2018). Parallelised Bayesian optimisation via Thompson sampling. In Storkey and Perez-Cruz (2018), pages 133–142.
- Kandasamy, K., Schneider, J., and Póczos, B. (2015). High Dimensional Bayesian Optimisation and Bandits

-
- via Additive Models. In Bach, F. and Blei, D., editors, *Proceedings of the 32nd International Conference on Machine Learning (ICML'15)*, volume 37, pages 295–304. Omnipress.
- Klein, A., Falkner, S., Bartels, S., Hennig, P., and Hutter, F. (2017). Fast bayesian hyperparameter optimization on large datasets. In *Electronic Journal of Statistics*, volume 11, page 4945–4968.
- Kuhnle, A., Schaarschmidt, M., and Fricke, K. (2017). Tensorforce: a tensorflow library for applied reinforcement learning. Web page.
- Lindauer, M., Eggenberger, K., Feurer, M., Biedenkapp, A., Deng, D., Benjamins, C., Sass, R., and Hutter, F. (2021). Smac3: A versatile bayesian optimization package for hyperparameter optimization.
- McLeod, M., Roberts, S. J., and Osborne, M. A. (2018). Optimization, fast and slow: Optimally switching between local and bayesian optimization. In Dy, J. G. and Krause, A., editors, *Proceedings of the 35th International Conference on Machine Learning, ICML 2018*, volume 80 of *Proceedings of Machine Learning Research*, pages 3440–3449. PMLR.
- Oh, C., Gavves, E., and Welling, M. (2018). BOCK : Bayesian Optimization with Cylindrical Kernels. In Dy and Krause (2018), pages 3865–3874.
- Pimenta, C., de Sá, A., Ochoa, G., and Pappa, G. (2020). Fitness landscape analysis of automated machine learning search spaces. In *Proceedings of Evolutionary Computation in Combinatorial Optimization*, pages 114–130. Springer.
- Pushak, Y. and Hoos, H. (2018). Algorithm configuration landscapes: - more benign than expected? In *Parallel Problem Solving from Nature - PPSN XV - 15th International Conference, Coimbra, Portugal, September 8-12, 2018, Proceedings, Part II*, pages 271–283. Springer.
- Salimbeni, H., Eleftheriadis, S., and Hensman, J. (2018). Natural gradients in practice: Non-conjugate variational inference in gaussian process models. In Storkey, A. and Perez-Cruz, F., editors, *Proceedings of the Twenty-First International Conference on Artificial Intelligence and Statistics*, volume 84 of *Proceedings of Machine Learning Research*, pages 689–697. PMLR.
- Schulman, J., Wolski, F., Dhariwal, P., Radford, A., and Klimov, O. (2017). Proximal policy optimization algorithms. *arXiv:1707.06347 [cs.LG]*.
- Shahriari, B., Swersky, K., Wang, Z., Adams, R., and de Freitas, N. (2016). Taking the human out of the loop: A review of Bayesian optimization. *Proceedings of the IEEE*, 104(1):148–175.
- Snelson, E. and Ghahramani, Z. (2006). Sparse gaussian processes using pseudo-inputs. In *Advances in Neural Information Processing Systems*, volume 18, pages 1257–1264. MIT Press.
- Snoek, J., Larochelle, H., and Adams, R. (2012). Practical Bayesian optimization of machine learning algorithms. In Bartlett, P., Pereira, F., Burges, C., Bottou, L., and Weinberger, K., editors, *Proceedings of the 26th International Conference on Advances in Neural Information Processing Systems (NeurIPS'12)*, pages 2960–2968.
- Storkey, A. and Perez-Cruz, F., editors (2018). *Proceedings of the 21st International Conference on Artificial Intelligence and Statistics (AISTATS)*, volume 84. Proceedings of Machine Learning Research.
- Surjanovic, S. and Bingham, D. (2013). Virtual library of simulation experiments: Test functions and datasets. Retrieved January 28, 2021, from <http://www.sfu.ca/~ssurjano>.
- Thornton, C., Hutter, F., Hoos, H., and Leyton-Brown, K. (2013). Auto-WEKA: combined selection and hyperparameter optimization of classification algorithms. In Dhillon, I., Koren, Y., Ghani, R., Senator, T., Bradley, P., Parekh, R., He, J., Grossman, R., and Uthurusamy, R., editors, *The 19th ACM SIGKDD International Conference on Knowledge Discovery and Data Mining (KDD'13)*, pages 847–855. ACM Press.
- Titsias, M. (2009). Variational learning of inducing variables in sparse gaussian processes. In van Dyk, D. and Welling, M., editors, *Proceedings of the Twelfth International Conference on Artificial Intelligence and Statistics*, volume 5 of *Proceedings of Machine Learning Research*, pages 567–574, Hilton Clearwater Beach Resort, Clearwater Beach, Florida USA. PMLR.
- Turner, R. (2019). The bayes opt benchmark documentation. <https://bayesmark.readthedocs.io/en/latest/>.
- Wan, X., Nguyen, V., Ha, H., Ru, B., Lu, C., and Osborne, M. A. (2021). Think global and act local: Bayesian optimisation over high-dimensional categorical and mixed search spaces.
- Wang, L., Fonseca, R., and Tian, Y. (2020). Learning search space partition for black-box optimization using monte carlo tree search. In *Advances in Neural Information Processing Systems 33: Annual Conference on Neural Information Processing Systems*.

Wang, Z., Gehring, C., Kohli, P., and Jegelka, S. (2018). Batched Large-scale Bayesian Optimization in High-dimensional Spaces. In Storkey and Perez-Cruz (2018), pages 745–754.

Wang, Z., Shakibi, B., Jin, L., and Freitas, N. (2014). Bayesian multi-scale optimistic optimization. In *Proceedings of the Seventeenth International Conference on Artificial Intelligence and Statistics, AISTATS 2014*, volume 33 of *JMLR Workshop and Conference Proceedings*, pages 1005–1014. JMLR.org.

A Algorithms to Extract Subregions

Algorithm 1: Subregion Selection with Random Forest

- 1: **Input:** Search Space $\mathcal{X} \in \mathbb{R}^n$; candidate selected by global Bayesian Optimization \mathbf{x}_g , random forest model \hat{f} with n_{tree} trees; minimal number of points stored in the subregion n_{min}
 - 2: **Output:** subregion \mathcal{X}_{sub} extracted from \mathcal{X}
 - 3: **Initialization:** $\mathcal{D}_{sub} \leftarrow \mathcal{X}$; a list of root nodes S of RF \hat{f} , a nodes indicator $I \leftarrow [False] * n_{trees}$ indicating that if we will stop deeper from the node.
 - 4: **while** no element in I is False **do**
 - 5: **for** each node $s_p \in S$ **do**
 - 6: $s'_p \leftarrow child(s_p)$ with $\mathbf{x}_g \in s'_p$
 - 7: Let $\mathcal{D}_{s'_p}$ be all observed points in s'_p
 - 8: **if** $|\mathcal{D}_{sub} \cap \mathcal{D}_{s'_p}| > n_{min}$ **then**
 - 9: $s \leftarrow s'$
 - 10: $\mathcal{D}_{sub} \leftarrow \mathcal{D}_{sub} \cap \mathcal{D}_{s'}$
 - 11: **else**
 - 12: $I_p \leftarrow True$
 - 13: **end if**
 - 14: **end for**
 - 15: **end while**
 - 16: **Return:** An extracted subregion \mathcal{X}_{sub}
-

B Implementation Details

We start with a Gaussian Process that is trained on all the previous evaluated data points until n_{min} points exist in the dataset. Then we start to extract a subregion, as described in Algorithm 1. It makes no sense to introduce LGPGA if the number of \mathbf{f}_0 is smaller than n_u . In such a case, we still train a full GP model on all the previously evaluated points but only optimize the acquisition function values in the subregion. If we have more observations, we apply LGPGA to reduce the potential computation time.

B.1 LGPGA Details

We train our LGPGA model with the following manner: we first train a GP model to fit \mathbf{f}_1 to acquire the kernel hyperparameters. Then we use this optimized kernel to initialize a sparse GP and keep its kernel hyperparameters fixed, i.e. we approximate \mathbf{f}_0 by only optimizing the position of the inducing points. The hyperparameters of LGPGA thus captures both \mathbf{f}_1 (the kernel hyperparameters) and \mathbf{f}_0 (the inducing points positions). We apply variational GP (Titsias, 2009; Hensman et al., 2013) to approximate \mathbf{f}_0 with its hyperparameters optimized with natural gradient descend Salimans et al. (2017). We train the sparse

GP to approximate the predictive variational evidence lower bound (ELBO), as proposed in Jankowiak et al. (2020). A further advantage of a variational GP is that it allows stochastic variational inference (SVI), i.e. we could scale variational GP to even larger dataset as the number of evaluations grows. However, in this paper, we only consider batch optimization.

We set number of inducing points to be at least $\min(2 \times n_{dims}, 10)$ and it grows linearly as number of total evaluations grows ($\min(\frac{n_p}{20})$ where \mathcal{D} denote all the previous evaluations) and up to 50 points.

B.2 BOinG+ Details

When working with larger budgets (e.g. larger than 500 evaluations), as Random Forest might converge to a local minimum, we combine TuRBO (Eriksson et al., 2019) and BOinG in the following ways: we start with BOinG and set a failure counter c_{fail} . We increase it every n_{dim} times when we have not found a better configuration or decrease it if a better configuration was found. The probability of switching to TuRBO is computed as:

$$p_{switch} = 0.1 * c_{fail} \quad (1)$$

As BOinG potentially acts as an exploitation mechanism, we will let TuRBO focus more on exploration: we randomly sample 20 configurations $\mathbf{X}_{random} \in \mathcal{X}$ and extract their subregions accordingly with Algorithm 1. We take the subspace \mathcal{X}_{sub} with the largest volume and build a TuRBO optimizer inside \mathcal{X}_{sub} . The TuRBO optimizer is initialized with the points inside this subspace. Eriksson et al. (2019) restarts TuRBO if the length of the subregion is smaller than 2^{-7} . We restart TuRBO if the length of the subregion is smaller than 2^{-4} instead to allow more repetitions. Similarly, we adjust the probability of switching to BOinG with Equation 1. However, if TuRBO finds a better configuration, we switch back directly to BOinG for further exploitation. Each time when we switch between BOinG and TuRBO, we halve their failure counts c_{fail} accordingly to avoid too frequent switching.

C Experiments Details

For Adult and Cartpole problems, we allow $2 \cdot n_{dims}$ initial points and they are initialized with a Sobol sequence, except for TuRBO and LA-MCTS. The deterministic Sobol sequence is not applicable to TuRBO and LA-MCTS since they require the randomness by initialization to restart with different points. All the optimizer runs are repeated 30 times.

For the CartPole benchmark, we optimized the reward value achieved by the agent after a maximum of 200

episodes or 6000 steps—whichever was reached first. The final performance is the mean reward of 20 episodes by the trained agent. To reduce the impact of noise, for each hyperparameter configuration, we repeatedly evaluate 9 runs and return the mean value of the final cost value.

Lunar Lander and Robot Pushing tasks are applied in Eriksson et al. (2019). We set the same search space as TuRBO did¹ due to the large amount of time required for each evaluation. We only run 20 repetitions for these two benchmarks. For the lunar lander problem, we allocate a budget of 1500 function evaluations and for robot pushing, a budget of 3000 function evaluations.

All the related data can be found under <https://figshare.com/s/757b2b74d77586690458>.

D Ablation Study

In this section, we first continue our ablation study in Section 4.3 of the main paper but on different tasks. Then we will discuss the choices that we adapted to different tasks.

D.1 Ablation Study on Adult

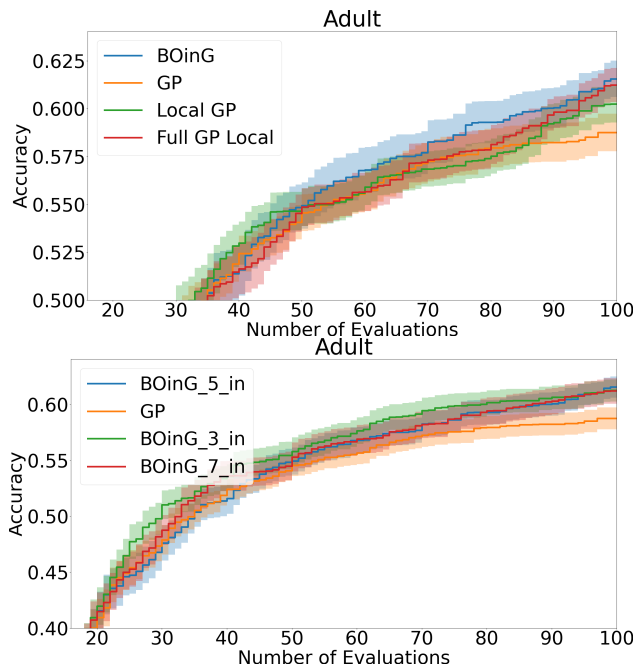


Figure 1: Ablation Study on LGPGA (Top) and n_{min} (Bottom) on the Adult task.

Figure 1 shows how different choices of GPs and n_{min} influences the optimization process on the Adult task. LGPGA and *full GP local* still outperform *Local GP*

and acquire similar final performance. However, different choices of n_{min} does not affect the performance on the Adult task too much, all the BOinG-variation has similar performance. This also indicates that the landscape of the target problem might also influence the final performance of the optimizer.

D.2 Ablation Study on the choice of acquisition function at the global level

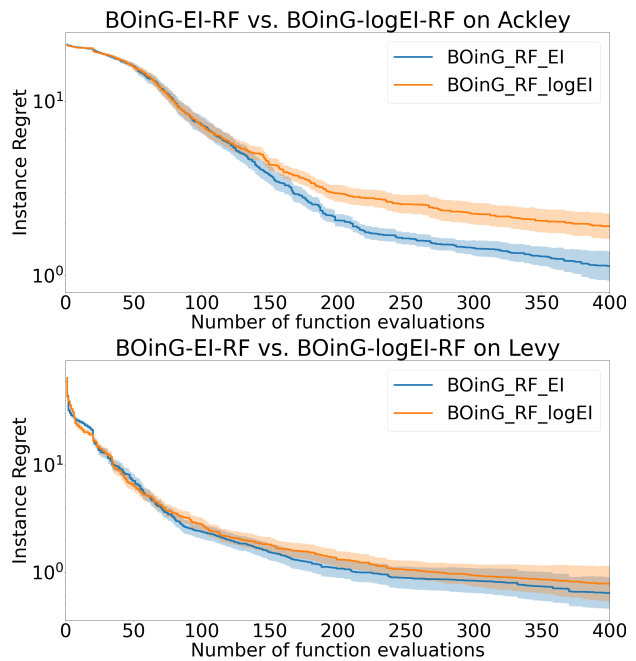


Figure 2: Ablation Study on the choice of the acquisition function at the global level on ackley (top) and levy (middle) function.

Instead of the default setting of logEI (Hutter et al., 2012), we apply vanilla EI as the acquisition function at the global level on synthetic functions. These synthetic functions usually do not fit the requirement of "heavy-tailed cost distributions" (Lindauer et al., 2021) and possess several local minima that an optimizer might easily fall into. Applying EI allows the optimizer to explore the unknown regions more and thus provides the optimizer a higher probability to find the global optimum. The result is illustrated in Figure 2. BOinG equipped with EI as the acquisition function at the global level generally has a better any time performance.

D.3 Ablation study on BOinG+

In Section 3.3, we proposed to randomly switch between BOinG and TuRBO depending on their results accordingly. Here we will study if BOinG+ achieves a better exploitation-exploration tradeoff than TuRBO. As we restart TuRBO earlier to allow more exploration,

¹<https://github.com/uber-research/TuRBO>

we first check if this strategy helps TuRBO to find a better configuration. According to Section 3.3, we restart TuRBO if the length of the subregion is smaller than 2^{-4} , called *TuRBO_4*. Additionally, we will study the extra benefit that BOinG+ brings to BOinG and TuRBO, we compare it with vanilla BOinG where BOinG never switches to TuRBO (*BOinG_Vanilla*) and a BOinG+ version where TuRBO never switches to BOinG (*RF_TuRBO*). The results are shown in Figure 3. Vanilla BOinG underperforms compared to the other variants. TuRBO_4 becomes more explorative in the very beginning but cannot dig deeper as it restarts too early and is outperformed by RF_TuRBO as it cannot capture the global data distribution. BOinG+ instead allows further exploitation and finds the best configuration in the end.

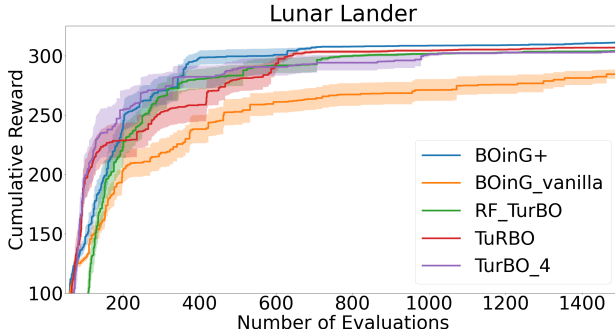


Figure 3: Ablation Study on BOinG+.

E Scalability

One drawback of a Gaussian Process is its cubic complexity with respect to the number of the points ever evaluated. Similar to other local BO approaches (Eriksson et al., 2019; Wang et al., 2018, 2020), our approach alleviates this problem by developing a model only with a subset of the previous evaluations. However, a local GP still scales cubically w.r.t. the number of points inside the subregion (and does not capture the overall trend). Hence the complexity of our algorithms mainly depends on the number of points inside the subregion.

E.1 Complexity of Partial Sparse GPs

Assuming that the size of \mathbf{f}_0 , \mathbf{f}_i and u are n_g , n_l and m respectively, the complexity of fitting a model in the first and second stages are $\mathcal{O}(m^2 n_g)$ and $\mathcal{O}((m + n_l)^3)$ respectively. Predicting the mean and variance takes the complexity of $\mathcal{O}(m + n_g)$ and $\mathcal{O}((m + n_l)^2)$. Normally we have $m \ll n_g \ll n_l$, although the posterior distribution needs to be computed twice, we can still save a lot of resources by introducing LGPGA without loss of precision. Additionally, a sparse GP can only be trained with \mathbf{f}_i and \mathbf{f}_0 jointly, which might underfit

\mathbf{f}_i . Later we will show how different components of LGPGA emphasise different parts of training data.

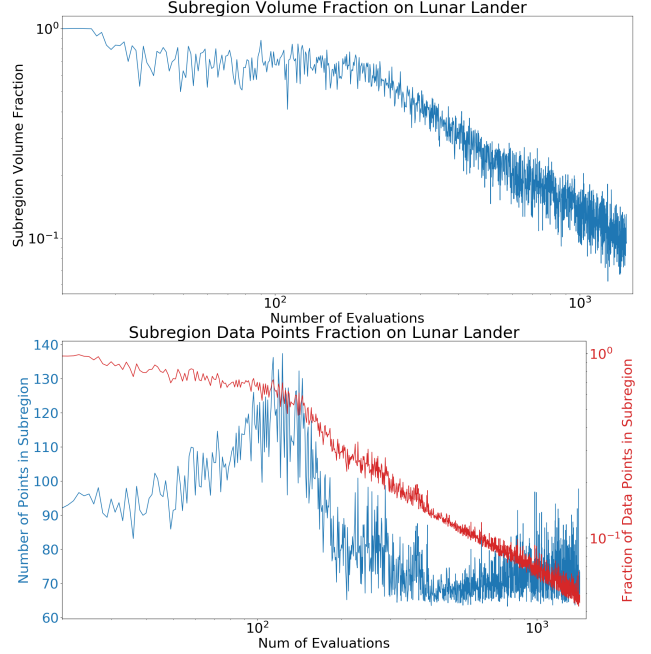


Figure 4: Top: fraction of subregion volume versus the entire region. Bottom: number of points inside subregion versus number of evaluated points.

Figure 4 illustrates how the number of data points varies as the number of evaluations grows. Here we take the evaluation result on the lunar lander problem as an example, where $n_{dims} = 14$ and thus the minimal number of points inside the subregion is 70. We could see that the number of points inside the subregion stays nearly constant as the number of evaluations grows. The subregion quickly shrinks after about 100 evaluations and hence our local model could focus more on the most promising region. However, this trend does not hold for the following evaluations. The subregion only shrinks smoothly in the following evaluations, which will prevent BOinG from converging to a local minimum too early.

Figure 5 illustrates the time spent for a BOinG iteration as the number of evaluations grows. Starting from the 200th evaluations on ackley 10D, BOinG takes less time in each iteration compared to a full GP. From the right plot in Figure 5, we could see that BOinG scales nearly linearly as the number of evaluations grows until up to 1500 evaluations.

Next we evaluate the saved resources and the additional overload that LGPGA brings to global and local GP models. Again, we train 3 different models on the data that we obtained when we optimize the hyperparameters on lunar task: full GP denotes a GP model that is trained on all the previous evaluated points; local GP

denotes a model that is trained only with the points inside the subregion; and finally our LGPGA model. Here, the GP’s hyperparameters are optimized with 10 repetitions. The result is illustrated in the top part of Figure 5. Compared to a full GP model, LGPGA requires much less resources and scales nearly linearly as the number of the previous evaluations grows.

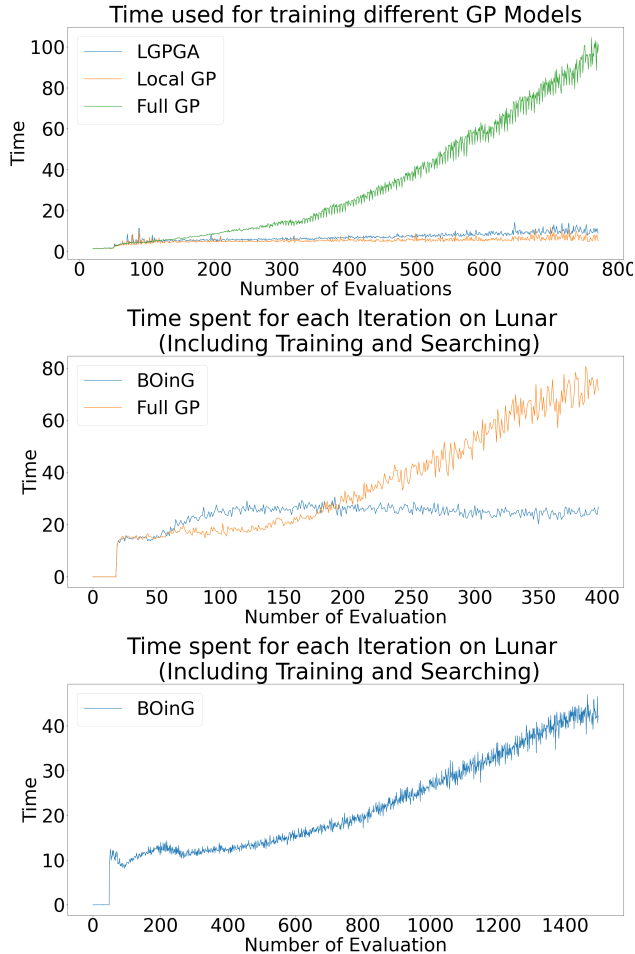


Figure 5: Scalability Analysis, we note that we optimize GP’s hyperparameters with L-BFGS (Liu and Nocedal, 1989) optimizer and repeat optimization for 10 repetitions with different initial points on Lunar Lander (14D). **Top:** time spent for training different GP models. **Middle:** Time Spent by BOinG and Full GP for each BO iterations on Ackley (10D). **Bottom:** Time Spent for each BO iterations on Lunar Lander (14D).

F How LGPGA Guides the Search in Subspaces

In Section 3.2, we used a toy example to show how LGPGA handles heteroscedastic noise. The data is generated according to Yuan and Wahba (2004) and

follows a normal distribution with mean: $\mu(x) = 2(\exp(-30(x - 1/4)^2) + \sin(\pi x^2))$ and variance $\sigma^2(x) = \exp(2 \sin(2\pi x))$. This distribution has low noise level with larger x values and high noise level with smaller x values. Here we only use our model to fit the distribution of the right side. We randomly sample 50 points from $[0, 1]$ and select the points indices from 35 to 45 as the points inside the subregion. The predicted mean and variances are illustrated in Figure 6. Fitting a GP on the entire data distribution will not exactly describe the noise on the right part of the data distribution. The GP fitting only the data points inside the subregion and our LGPGA describe better the heteroscedastic noise inside the subregion.

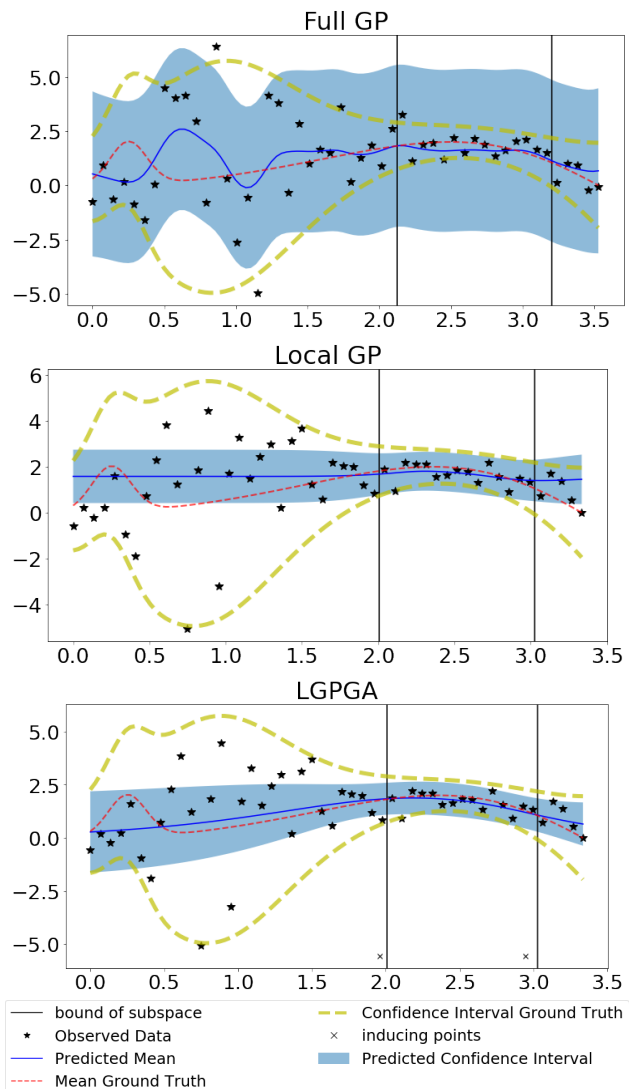


Figure 6: Predicted mean and variance of a **Top:** full GP **Middle:** local GP **Bottom:** LGPGA

Additionally, we illustrate how LGPGA influences the acquisition function value landscape and guides the search.

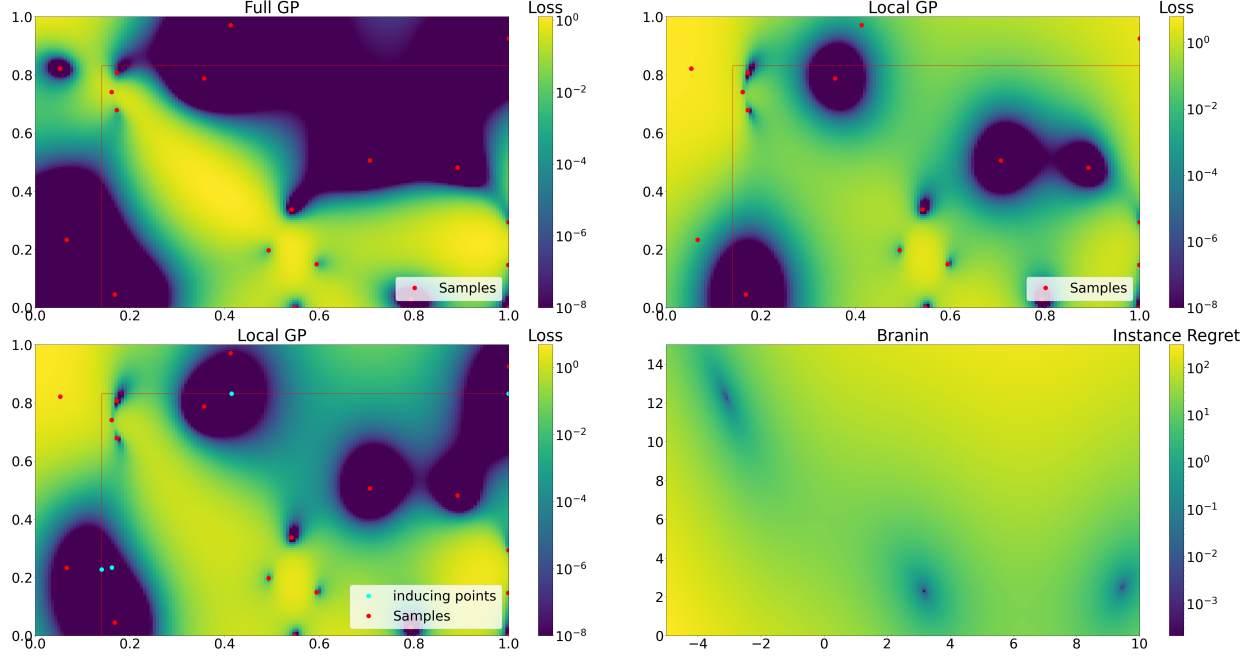


Figure 7: Predicted EI value of different GP models, red rectangles are the boundary of the subregion. From top left to bottom right: a GP model that is trained on all the previous evaluations; a GP model that is trained to only fit the distribution inside the subregion (the red rectangle); a LGPGA model trained with all the previous evaluations; the loss landscape of branin function.

Similar to section E, we train full GP, local GP and LGPGA on the same data distribution. The subregion is bounded by the rectangle. Without knowing the information of the points outside the subregion, the local GP will have a large chance to sample the points on the top right of the subregion for exploration. However, the high loss of the samples on the top right indicates that it might not be a good choice to sample a new point in this direction, as illustrated by the acquisition value loss landscape of the full GP model. However, LGPGA optimizes its inducing points to approximate the distribution outside the subregion and we see that two inducing points are located on the bottom left of the subregion while another two lay on the top side. Thus we could avoid unnecessary exploration on the bottom left and focus more on the region near the optimum or the direction that is still not fully explored.

G Will BOinG+ Give Better Suggestions compared to TuRBO?

BOinG+ switches between TuRBO and BOinG randomly according to their failure counts. In the ablation study, we show that BOinG+ has a better final performance compared to different variation of TuRBO. However, it is still unclear where the incumbent configuration comes from, i.e., if BOinG+ works as we expect: explore with TuRBO and exploit with BOinG?

To answer this question, we show the fraction of the incumbents' origin as the number of evaluations grows on the two tasks where BOinG+ is applied.

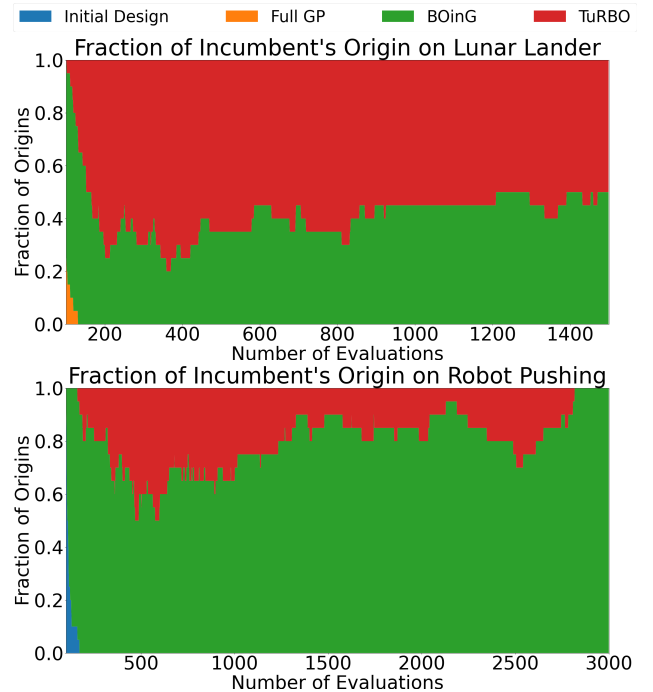


Figure 8: Share of different incumbents' origins

The results are shown in Figure 8. Depending on the

task, the performances are quite different. This shows that BOinG+ could adjust to different sorts of landscapes and not get stuck at one single optimizer. The share of TuRBO reaches peak at roughly 500 evaluations and then more incumbents are suggested by BOinG. Thus, as expected, TuRBO explores more in the mid term of the optimization process and thus finds more incumbents during this period; while BOinG exploits more in the most promising regions and thus gives more incumbents at the end.

References

- Eriksson, D., Pearce, M., Gardner, J., Turner, R., and Poloczek, M. (2019). Scalable global optimization via local bayesian optimization. In *Advances in Neural Information Processing Systems*, volume 32, pages 5496–5507.
- Hensman, J., Fusi, N., and Lawrence, N. D. (2013). Gaussian processes for big data. In *Proceedings of the Twenty-Ninth Conference on Uncertainty in Artificial Intelligence*, UAI’13, page 282–290, Arlington, Virginia, USA. AUAI Press.
- Hutter, F., Hoos, H., and Leyton-Brown, K. (2012). Parallel algorithm configuration. In Hamadi, Y. and Schoenauer, M., editors, *Proceedings of the Sixth International Conference on Learning and Intelligent Optimization (LION’12)*, volume 7219 of *Lecture Notes in Computer Science*, pages 55–70. Springer.
- Jankowiak, M., Pleiss, G., and Gardner, J. (2020). Parametric Gaussian process regressors. In III, H. D. and Singh, A., editors, *Proceedings of the 37th International Conference on Machine Learning*, volume 119 of *Proceedings of Machine Learning Research*, pages 4702–4712. PMLR.
- Lindauer, M., Eggenberger, K., Feurer, M., Biedenkapp, A., Deng, D., Benjamins, C., Sass, R., and Hutter, F. (2021). Smac3: A versatile bayesian optimization package for hyperparameter optimization.
- Liu, D. C. and Nocedal, J. (1989). On the limited memory BFGS method for large scale optimization. *Math. Program.*, 45(1-3):503–528.
- Salimans, T., Ho, J., Chen, X., and Sutskever, I. (2017). Evolution strategies as a scalable alternative to reinforcement learning. *arXiv:1703.03864 [stat.ML]*.
- Storkey, A. and Perez-Cruz, F., editors (2018). *Proceedings of the 21st International Conference on Artificial Intelligence and Statistics (AISTATS)*, volume 84. *Proceedings of Machine Learning Research*.
- Titsias, M. (2009). Variational learning of inducing variables in sparse gaussian processes. In van Dyk, D. and Welling, M., editors, *Proceedings of the Twelfth International Conference on Artificial Intelligence and Statistics*, volume 5 of *Proceedings of Machine Learning Research*, pages 567–574, Hilton Clearwater Beach Resort, Clearwater Beach, Florida USA. PMLR.
- Wang, L., Fonseca, R., and Tian, Y. (2020). Learning search space partition for black-box optimization using monte carlo tree search. In *Advances in Neural Information Processing Systems 33: Annual Conference on Neural Information Processing Systems*.
- Wang, Z., Gehring, C., Kohli, P., and Jegelka, S. (2018). Batched Large-scale Bayesian Optimization in High-dimensional Spaces. In Storkey and Perez-Cruz (2018), pages 745–754.
- Yuan, M. and Wahba, G. (2004). Doubly penalized likelihood estimator in heteroscedastic regression. *Statistics & Probability Letters*, 69(1):11 – 20.